Malays. J. Bioeng. Technol. Vol. 1, No. 1, (2024): 66-81
https://doi.org/10.70464/mjbet.v1i1.1274

MALAYSIAN JOURNAL OF BIOENGINEERING AND TECHNOLOGY

MJBeT Malaysian Journal of Bioengineering and Technology

Optimizing Oil Palm Tree Inventory Management with Advanced Drone-Based Image Recognition Techniques

Intan Noradybah Md Rodi, Shaparas Daliman*

Faculty of Earth Science, Universiti Malaysia Kelantan, Jeli Campus, 17600 Jeli, Kelantan, Malaysia.

**Corresponding author: shaparas@umk.edu.my*

ARTICLE INFO

Received: 24 March 2024
Accepted: 20 April 2024
Online: 22 June 2024
eISSN: 3036-017X

ABSTRACT

Oil palm tree plantations are a crucial source of vegetable oil for various industries, playing a significant role in the global economy. One key aspect of plantation management is accurate inventory management of oil palm trees, which involves the detection and counting of individual trees. Traditional inventory management methods for oil palm trees rely on ground-based manual measurements, which are time-consuming, labor-intensive, and prone to errors. However, accurate and efficient detection and counting of oil palm trees from drone images remain challenging due to the complex and variable nature of the plantation environment. Drone-based remote sensing has emerged as a promising alternative for inventory management in recent years. In this study, a novel approach to enhance the accuracy and efficiency of oil palm tree detection and counting using advanced drone-based image recognition techniques is proposed. The research discusses a novel image recognition technique that uses a custom GLCM, Haar Wavelet, and template matching to detect and count oil palm trees from drone images. The proposed approach outperformed traditional machine learning techniques and achieved a high accuracy of 83.75% and 86.9% in detecting individual oil palm trees in Jeli and Keratong, respectively. Haar Wavelet proves this algorithm achieves the highest overall accuracy. Additionally, eight statistical parameters can manipulate the GLCM, while offset parameters can boost accuracy for various applications or methods. The study highlights the potential of advanced drone-based image recognition techniques for optimizing plantation management and contributing to sustainable production practices.

Keywords: Oil palm plantation; Gray-Level Co-occurrence Matrix (GLCM); Haar Wavelet; Support Vector Machine; drone images

1. Introduction

Malaysia is one of the top exporters of oil palm, accounting for 28.6% of the global market share in 2018, second only to Indonesia. The Malaysian Palm Oil Council (MPOC) [1] reports that Malaysia is one of the largest producers and exporters of palm oil in the world, accounting for 11% of the world's oils and fats production and 27% of export trade of oils and fats. The industry provides employment to more than half a million people and livelihood to an estimated one million people.

Tree plantation identification is crucial for plantation management, environmental management, biodiversity monitoring, and many other applications [2]. Accurate inventories and monitoring of oil palm estates can be challenging and critical for plantation management and plant area expansion. Manual field-based tree counting is time-consuming and high-cost, making it almost impossible to manage oil palm estates manually. Developing an easier, simpler, and cheaper method for tree counting is needed. Conventional methods for tree counting can be carried out by manually marking images or carrying out field surveying using GPS to collect the positions of oil palm trees and display their position on the image [3].

There is no doubt that, with the development of image recognition, human life has been eased, especially in monitoring and observation activities in crop management. Aiming to provide a solution for the problem in oil palm monitoring, unmanned aerial vehicles (UAV) are effectively being used for plantation monitoring and will be paired with developed sensors and computing-based methods to perform automated image analysis. The result would provide labor support, and the production can be increased with high accuracy of monitoring activities.

Drones have also been used to count oil palm trees. Kattenborn et. al [4] used photogrammetric point clouds from UAV-based for automatic single palm tree detection in plantations. Among the software used are VisualSFM and 3DF Lapyx to calculate internal camera parameters. Plus, airborne hyperspectral imagery was used in the tree counting study. Shafri et al. [5] proposed a method for detecting oil palm trees by using airborne hyperspectral imagery, which provides rich information to remove non-oil palm features from the image. This study reported that using high spatial resolution remote sensing imagery allows them to handle the oil palm tree detection problem and proposed a new algorithm. Szantoi et al. [6] used Sobel edge detection and several color band combinations to detect trees from very high spatial resolution (0.3m) aerial imagery. Katoh and Gougeon [7] improve the precision of tree counting by combining tree detection with crown delineation and classification on homogeneity by using multispectral airborne digital data.

Studies on determining and counting trees or objects have been conducted by several researchers, including Bazi et al. [8], Gong et al. [9], Christophe and Inglada [10], and Vibha et al. [11] using different kinds of images. An increasing number of oil palm research-related studies show this field has captured the interest and awareness of researchers worldwide. However, a study on identifying the oil palm tree based on drone images using deep learning is still very limited. Only Li et al. [12] and Mubin et al. [13] have conducted studies using deep learning methods using QuickBird images and WorldView-3 images, respectively. Both studies show high accuracy achievement in identifying the oil palm trees using deep learning methods. Thus, this research would be the first to implement and improve the technique of deep learning image recognition for oil palm plantations using drone-based remote sensing images. In this research, an improvement in the technique for data acquisition and image processing was developed utilizing multispectral imaging based on drone and deep learning convolutional neural networks to evaluate the phenotypic characteristics of oil palm crops.

The study aims to develop an automated image recognition technique for oil palm tree area recognition based on the highest accuracy obtained in oil palm tree recognition. By using drone-based remote sensing images, enhanced tree recognition techniques were established. The oil palm tree recognition techniques produced were also used to count the number of oil palm trees in oil palm plantations in Jeli, Kelantan, and Keratong, Pahang.

1.1 Oil Palm Industry

The oil palm, also known scientifically as *Elaeis guineensis*, is a native of West Africa, where evidence of its use as a basic food yield dates as far back as 5,000 years. Oil palm is a monoecious crop. It consisted of both male and female flowers on the same tree. Each tree produces a close-packed cluster of about 1000 to 3000 fruit per cluster. The shape of the fruits is spherical or elongated. The fruit is blackish purple, and when it rips, it turns to reddish-orange.

It was first brought into Malaysia by the British in the early 1870s as a decorative plant. In 1917, Tennamaran Estate in Selangor was the first estate to be established as the first commercial planting, which was the pioneer for the huge oil palm plantations and the palm oil industry in Malaysia. The production of oil palm skyrocketed in the early 1960s under the government's agricultural diversification program, which was initiated to find another economic source

eISSN Number: 3036-017X

in order to overcome the economic dependence on rubber and tin. In Malaysia, oil palm plantation is mainly supported by the estate management system and smallholder schemes.

Palm oil is being used globally. Although some countries use unrefined palm oil, refined oils are used every day in Malaysia. Palm oil is plentiful, healthful, relatively cheap, and suitable for most food products. Hence, it is a high-demand industry across the globe. Other than that, oil palm tree is used to create a diversity of products such as plywood, furniture, and many more. Palm oil is also used in making soaps, cosmetics, candles, biofuels, and lubricating greases. The oils are also used to process tinplate and cover iron plates.

1.2 Effect of the Oil Palm Industry on the Economy

Oil palm trees start producing fruits after 30 months of planting on the field and will keep producing for 20 to 30 years. Hence, palm oil is consistent in providing oil to the demand. Now, in Malaysia, 5.8 million hectares of land are assigned for oil palm production, which can produce approximately 19.5 million tonnes in 2018, generating export earnings of RM 67.5 billion [14]. In 2017, the largest contributor to Malaysia's gross domestic product (GDP) in the agricultural field was palm oil, with a gross of RM 44.8 billion or 3.8% of the GDP contribution. Malaysia is one of the top producers and exporters across the globe, contributing to 11% of the cultivation of oil and fat around the world and 27% of the export trade of oils and fats [1].

Malaysia is focusing on 12 national key economic areas (NKEA) to assist its economy, and it is also aiming to reach a high-income status by 2020. Under NKEA, the palm oil industry is targeting to contribute RM 178 billion to Gross National Income (GNI) [15]. The palm oil industry in Malaysia plays a vital role in reducing poverty and in the movement of workers from village to city. The industry has created job opportunities, built infrastructure, and contributed to stability in the communities.

1.3 Remote Sensing

Remote sensing is a process of acquiring information about the Earth's surface without actually being in contact with it. This is done by sensing and recording reflected or emitted energy and processing, analyzing, and applying that information [16]. Remote sensing techniques for forest cover change detection and monitoring have been used to assess the differences in forest cover over two or more time periods caused by environmental conditions and human actions. Remote sensing and Geographical Information Systems (GIS) are practical tools for estimating and confirming ecosystem changes arising from forest use and forest management interference.

Remote sensing data provides a means of quickly identifying and delineating various forest types, which will be difficult and time-consuming if traditional ground surveys are used. Data is available at various scales and resolutions to satisfy local or regional demands. Species identification can be performed with the interpretation of multi-spectral, hyper-spectral, or air photo data. Both imagery and the extracted information can be incorporated into a GIS to analyze further slopes, ownership boundaries, or roads [16]. Remote sensing satellite is a widely used technique to study vegetation cover. Normally, data about Earth's features is acquired either from air, which is aerial photography, or from space, which is satellite imagery. Aerial photographs are in analog form, while images are basically in digital form.

Remote sensing is based on the measurement of electromagnetic energy. The remote sensing sensor measures the energy that is reflected or backscattered by the earth's surface. The measured energy is converted and stored as a digital number (DN) value, which ranges from 0 to 255. Each pixel has a single DN value. Most sensors measure reflected sunlight, which is passive remote sensing. However, some sensors detect energy emitted by the earth itself or provide their own source of energy, which is active remote sensing [17].

1.3.1 Satellite

A satellite is an object in space that orbits around a larger object. Satellites are categorized into two, which are natural and artificial. Natural satellites, such as the moon, circle the Earth, while artificial satellites, such as the International Space Station (ISS), circle the Earth. The first artificial satellite in the world was launched by Russia in

eISSN Number: 3036-017X

1957. Sputnik 1, launched by Russia, has been an initiator in the space race as a lot of countries built their own satellite. Now, a huge number of satellites and space stations have been launched and assembled in orbit.

1.3.2 Unmanned Aerial Vehicle

Unmanned aerial vehicles (UAVs) can make a practical map. Light, handy drones are rapidly being deployed. They convey lightweight digital cameras that can take great-quality pictures. These cameras can be set to capture images at basic intervals, and digital memory is economical and unlimited [18]. After securing the pictures, the pictures can be stitched into geo-corrected orthomosaics. They can be geometrically corrected to a uniform scale, adapted so that they comply with a typical geographical coordinate system, and stitched together.

There are different types of maps that are produced by UAVs, which are geographically ortho-rectified 2D maps, elevation models, thermal maps, and 3D maps or models [19]. The 2D map is the most familiar product made from imagery gathered from UAVs. The easiest approach to make a mosaic from aerial imagery is by utilizing photograph stitching software such as Agisoft software. It blends a series of overlapping aerial images into a specific photo. But, without a geometric adjustment, it is hard to measure distance accurately. Geometric adjustment is a procedure that separates the angle misinterpretation from the aerial photograph. Images that have been knitted are continuous along the boundaries. However, it does not have perspective distortion corrected. It is challenging to determine the geographical references accurately in the absence of a ground control point and over-viewed location, which is recognizable in the image.

1.4 Tree Detection and Counting

1.4.1 Texture

Texture is a feature used to construct and sort images into points of interest. It provides information about the image regarding color or intensity spatial structure. In image recognition, texture classification is one of the difficulties, and the problem lies in distinguishing between the textures [20]. Texture analysis had two primary issues: texture segmentation and texture classification. Texture is one of the crucial techniques used in image processing for the assessment of texture. Its main features are separation, discrimination, identification, classification, segmentation, and supervised classification.

1.4.2 Gray Level Co-Occurrence Matrix

Gray Level Co-occurrence Matrix, also known as GLCM, is one of the texture analysis methods where it studies the relationship between 2 pixels. Texture characteristics are determined in statistical texture analysis from the statistical distribution of observed combinations of intensities at defined positions relative to each other in the image [21]. The probability of GLCM can be defined as the number of times this result appears, divided by the total of potential outcomes. This is only an estimation since a definite likelihood would involve cumulative values, so it can also be a specific frequency value that can only be integer values. So this technique is called matrix normalization [22]. Standardization requires dividing values by a number. It varies from the likelihood scientifically. It can be expressed scientifically by Normalization equation:

$$P_{i,j} = \frac{V_{i,j}}{\sum_{i,j=0}^{N-1} V_{i,j}} \tag{1}$$

Where:

i is the row number and j is the column number.
V is the value in the cell i, j of the image window.
P_{ij} is the probability value recorded for the cell.
N is the number of rows or columns.

eISSN Number: 3036-017X

1.4.3 Haar Wavelet

Haar Wavelet is a sequence of functions and is also known as the simplest wavelet ever. It is often used in image processing, where excess data requires a huge storage space. Haar Wavelet is an orthonormal interval system [0,1]. It is a series consisting of supported functions for small sub-intervals of length [0,1].

Since Haar Wavelet is a simple wavelet, the functional limitation is not continuous, so it cannot be distinguished. However, Haar Wavelet can also benefit the study of spontaneous transition. In order to compress one- and two-dimensional signals, Haar Wavelet is used. Haar Wavelet can be described as below:

$$\varphi = \begin{cases} 1 \\ \quad 0 \le x \le 1 \\ 0 \quad otherwise, \end{cases} \tag{2}$$

1.4.4 Template Matching

In image processing, template matching is a significant subject in the field as it is one of the methods for the key issue, which is determining the area of interest. The subject identifies whether the object of interest is in the image analyzed. Template Matching is widely used in many fields, including image recognition, mapping and monitoring, image stitching, and medical imaging. Template Matching is made of two primary elements, which are the source image and the testing set or patch [23].

It is classified into two categories: template-based and feature-based. Since they run directly on image pixels, the template-based method can be efficient for structures with few features or where the majority of the template image acts as the corresponding image. The intensity values of both the image and the template are used to determine similarity. Next, when there is more similarity between the source and template images in terms of features and control points, the feature-based method is used. Neural Networks and Deep Learning classifiers such as ResNet are used in this method by processing them through multiple hidden layers, each creating a variable with image classification data [24].

1.4.5 Support Vector Machine (SVM)

The support vector machine (SVM) is a neural network-based model that includes classification methods for problems with the classification of two classes. Because of the linear distinction concept, there are several potential hyperplanes that could be selected to distinguish the two types of data points. Hyperplanes are decision borders that clearly distinguish data points. Data points falling on either side of the hyperplane can be assigned to various groups. The distance from any set between both the hyperplane and the closest data point is defined as the margin. Hence, SVM is often referred to as the maximum margin classifier. The purpose is to identify a hyperplane with the maximum possible margin between the hyperplane and some point within the training set, which is highly important as it will increase the accuracy of the classification of new data.

Other than linear classification, SVM can effectively perform non-linear classifications by using the kernel trick, which indirectly maps their inputs into high-dimensional feature spaces. There are various types of kernels. However, the most used is the polynomial kernel and the radial basis function (RBF). The polynomial kernel focuses not only on the given characteristics of the input samples to determine their likeness but also on the combinations of the input samples. RBF kernels are similar to Gaussian distribution, where it measures the relation and distance between two points.

SVM can be beneficial to use in image recognition as it is efficient in high-dimensional structures and even in circumstances where the dimension number is larger than the sample size. SVM is also storage effective as it uses a subset of the training set in the support vector. For the decision function, various kernel functions may be defined. Hence, SVM is versatile as it can provide standard kernels as well as custom kernels. Nevertheless, SVM can't be used in larger training sets as its training time with SVM can take longer. SVM is also not practical on datasets with distortion, especially with overlapping classes.

eISSN Number: 3036-017X

1.5 Application of Unmanned Aerial Vehicle (UAV) on Oil Palm Plantation

Remote sensing research has been a rise in the field of oil palm plantation. Enforcing unmanned aerial vehicles (UAVs) in environmental and scientific research fields is already a technology that will help to accelerate even more developments throughout the future. However, UAVs are now a new method that has been used widely in the oil palm industry in the last few years. It benefits the sector from added values such as flexibility, low cost, reliability, and effectiveness in the timely supply of high-resolution data [25]. Nevertheless, UAVs currently have limited flight times and payload size, restricting the possible range of operations and the type of sensors that can be carried. The image is mainly based on technologies such as red, green, blue (RGB), multi-spectral, and thermal infrared. LiDAR sensors are widely used to enhance the assessment of particular plant's characteristics [26].

UAVs can help sustainable oil palm plantation practices in a few ways. Firstly, UAVs are effective when it comes to monitoring and surveying. Palm oil monitoring can be conducted for numerous reasons, such as tree counting, area of distribution, and many more. UAVs are able to obtain reliable imagery and turn it into a detailed map that consists of topography, height, terrain, and the like. It will be a huge help in replanting and preparing crop arrangements. This aid can ensure optimum returns and income while keeping the health of the environment on track. By implementing UAV, main areas with a high probability of land movement can also be established, and a mitigative plan can be introduced before it becomes a high risk and affects the crops and environment in the area.

2. Materials and Methods

2.1 Study Area

The study areas of this research focused on the comparison of small-scale oil palm plantations and big-scale oil palm plantations. The small-scale oil palm plantation area is located in Jeli, Kelantan, while the big-scale oil palm plantation is located in Keratong, Pahang.

2.1.1 Jeli, Kelantan

The study of oil palm tree recognition was conducted near Bandar Jeli, 17600 Jeli, Kelantan. The oil palm plantation is located at 5°42'34.3"N 101°50'41.9"E. The flying altitude of the drone is 54.8 m. The coverage area is around 0.0227 km² (Fig. 1).

Fig. 1: The location of the study site of the oil palm plantation near Bandar Jeli

2.1.2 Keratong, Pahang

The second study area is Keratong, Pahang. The data was retrieved from Malaysian Palm Oil Berhad (MPOB) which is located at 2°47'47.62"N 102°55'7.97"E. The coverage area is around 0.5 km^2 (Fig 2).

eISSN Number: 3036-017X

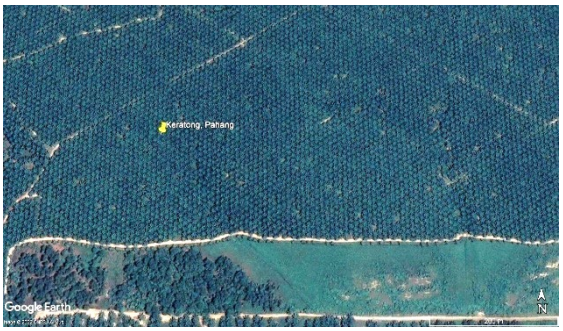

Fig. 2: The location of the study site of the oil palm plantation at Keratong

2.2 Data Acquisition

This study used images from an optical drone with three bands: red, green, and blue (RGB) bands. The type of drone used is Parrot ANAFI. The captured images were collected to be analyzed, and a structured set of databases from oil palm trees was developed using drone images.

2.2.1 Drone Images

The drone images of oil palm plantations have been stitched by using Agisoft Software, and an orthomosaic photos were produced (Fig. 3 and Fig. 4).

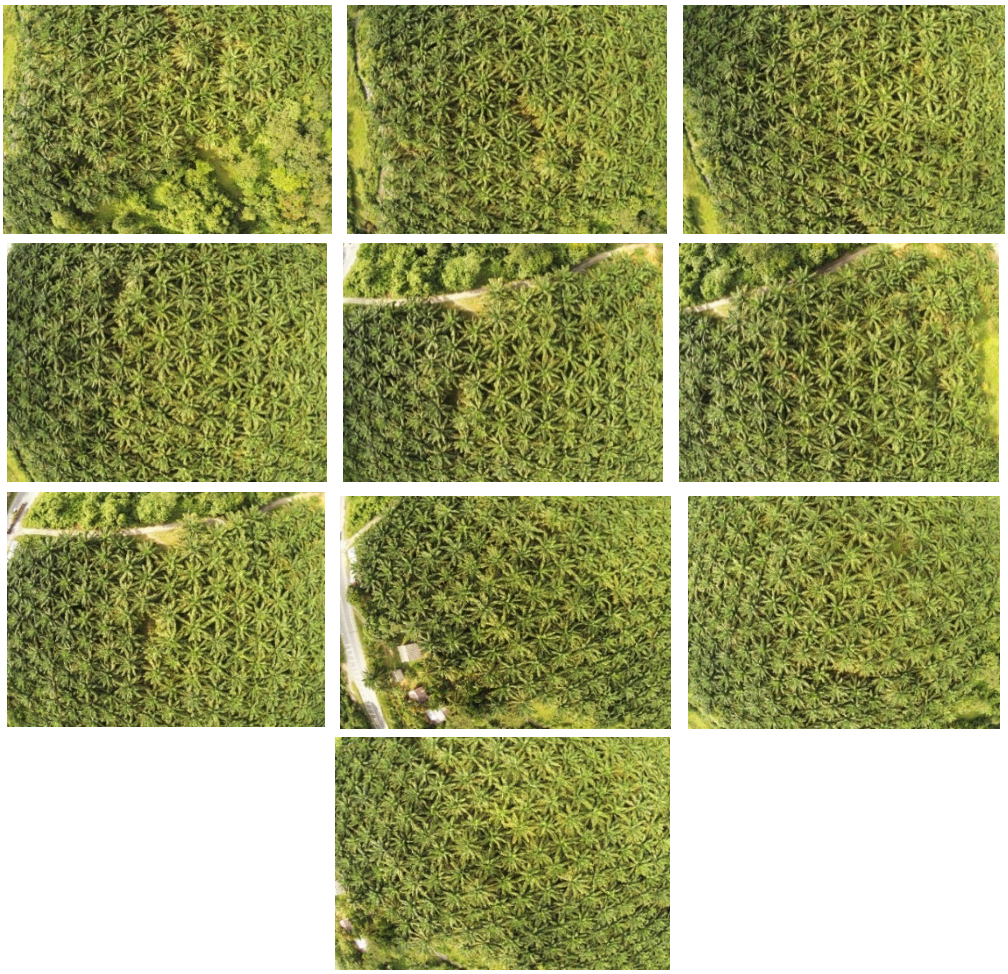

Fig. 3: Drone images of Jeli oil palm plantation

eISSN Number: 3036-017X

Fig. 4: Drone image of Keratong oil palm plantation

2.3 Data Processing and Analysis

There are three main algorithms involved in this work, which are the Gray-Level Co-Occurrence Matrix (GLCM), Haar Wavelet, and template matching, which has been used in Eq. (7). For GLCM, there are eight parameters that need to be manipulated to determine which parameters gives highest impact on tree counting.

2.3.1 Gray-Level Co-Occurrence Matrix (GLCM)

GLCM is a method of extracting second-order statistical texture features, a matrix where the number of rows and columns is equal to the number of gray levels, G, in the image. According to Eq. (8), GLCM can be defined as a higher-order set of texture measures based on brightness value spatial-dependency gray-level co-occurrence matrix (GLCM) has been widely used in image processing for remote sensing applications.

$$C_{i,j} = \sum_{x=0}^{M-1} \sum_{y=0}^{N-1} P\{I(x,y) = i \,\&\, I(x \pm d\emptyset_1, y \pm d\emptyset_2 = j)\} \quad (3)$$

Where if the argument is true, it will become 0; otherwise, Among 14 texture features described in Eq. (9) for each of GLCM, we have selected the following eight for our analysis which were contrast (CON), correlation (CORR), dissimilarity (DISS), energy (ENE), entropy (ENT), homogeneity (HOM), mean (MEAN) and variance (VAR):

$$CON = \sum_i \sum_j (i-j)^2 c(i,j) \quad (4)$$

$$CORR = \sum_i \sum_j (i-u_x)\big(j-u_y\big)\, c(i,j) / \big(\sigma_x \sigma_y\big) \quad (5)$$

$$DISS = \sum_i \sum_j |i-j| c(i,j) \quad (6)$$

$$ENE = \sum_i \sum_j \big(c(i,j)\big)^2 \quad (7)$$

$$ENT = -\sum_i \sum_j log\big(c(i,j)\big) c(i,j) \quad (8)$$

$$HOM = \sum_i \sum_j \frac{1}{1+(i-j)^2} c(i,j) \quad (9)$$

$$MEAN = \sum_{i=2} i \cdot c_{x+y}(i) \quad (10)$$

$$VAR = \sum_i \sum_j c(i,j)(i-\mu)^2 \quad (11)$$

Besides these eight statistics parameters, the offsets are also manipulated to see the effects of angle and direction in tree detection. Offset is a p-by-2 array of integers specifying the distance, *d*, between the pixel of interest and its neighbor. In this study, the GLCM parameters have been measured on five different distances, *d* of 1, 2, 3, 4, and 5 pixels spacing, and three different directions, ∅ of 0°, 45° and 90°. Then, by taking the average of measurement based on these ∅ only the eight texture features are calculated.

eISSN Number: 3036-017X

2.3.2 Haar Wavelet

Wavelet is a finite-energy function with localization properties that can be used efficiently to represent transient signals. The wavelet transform can be interpreted as a decomposition of the original signal into a set of independent frequency channels. Window function of wavelet transform:

$$\psi_{ab}(t) \triangleq \frac{1}{\sqrt{a}} \Psi\left(\frac{t-b}{a}\right) \tag{12}$$

The technical disadvantage of the Haar wavelet is that it is not continuous and, therefore not differentiable. This property can, however, be an advantage for the analysis of signals with sudden transitions, such as monitoring of tool failure in machines. The Haar wavelet's mother wavelet function can be described as

$$\psi(t) = \begin{cases} 1 & 0 \le t < \frac{1}{2}, \\ -1 & \frac{1}{2} \le t < 1, \\ 0 & \text{otherwise.} \end{cases} \tag{13}$$

Haar wavelet scaling function can be described as

$$\phi(t) = \begin{cases} 1 & 0 \le t < 1, \\ 0 & \text{otherwise.} \end{cases} \tag{14}$$

2.3.3 Template Matching

The critical idea of template matching was to compare a small portion of an image to be detected against all local regions in the image by cross-correlate with a filter Eq. (7). The best linear operator of the filter for finding an image patch is essentially the patch itself. The matching process moves the template image to all possible positions in the target image and computes a numerical index that indicates how well the template matches the image in that position. The numerical index can be determined by the strength of the linear association of template, t, with the target image, I, where the cross-correlation, C_{tI} has been used:

$$C_{tI} = \sum_m \sum_n t(m,n) I(m,n) \tag{15}$$

However, this raw cross-correlation is higher only when darker parts of the template overlap with darker parts of the image and brighter parts of the template overlap with brighter parts of the image. This will lead to different scores if they match the illumination intensities of the same image. In solving the different intensity images, both the template's pixels and the target image have to be normalized as follows:

$$\hat{t} = \frac{t-\bar{t}}{\sum(t-\bar{t})^2}, \hat{I} = \frac{I-\bar{I}}{\sum(I-\bar{I})^2} \tag{16}$$

and the raw cross-correlation in Eq. (17) will become the normalized cross-correlation, r as follows:

$$r = \frac{\sum_m \sum_n (t_{mn}-\bar{t})(I_{mn}-\bar{I})}{\sqrt{(\sum_m \sum_n (t_{mn}-\bar{t})^2)(\sum_m \sum_n (I_{mn}-\bar{I})^2)}} \tag{17}$$

3. Results and Discussions

3.1 Development of Database of Oil Palm Tree

The drone images of both oil palm plantations were analyzed, where they were classified on the basis of oil palm trees and non-oil palm trees. Based on the drone images, the characteristics of each type of oil palm can be determined from its crown. The characteristics of oil palm crowns are that they basically look like flower petals [27]. The patterns of crowns are used to mark the oil palm tree and non-oil palm tree. The database of oil palm trees based on the drone images is displayed in Fig. 5 and 6.

eISSN Number: 3036-017X

Fig. 5: oil palm tree (red mark) and non-oil palm tree (blue mark) in Jeli

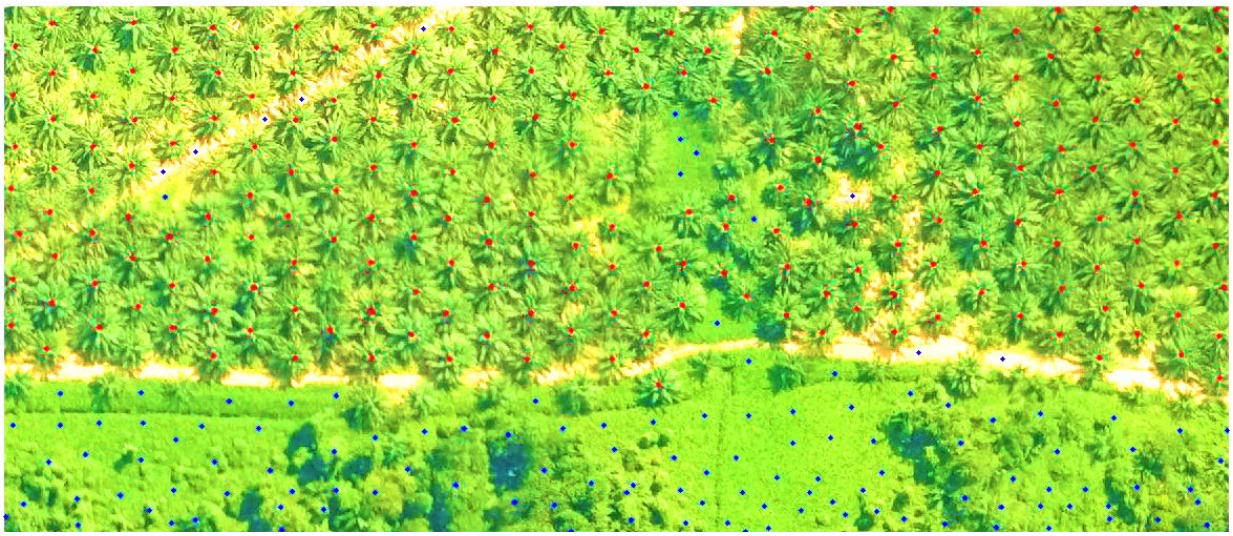

Fig. 6: The location of oil palm tree (red mark) and non-oil palm tree (blue mark) in Keratong

Table 1 shows the marking point for both oil palm and non-oil palm trees at Jeli and Keratong oil palm plantations. The total for oil palm trees for Jeli and Keratong plantations is 764 points and 2822 points, respectively. The total non-oil palm for Jeli is 608 points, while for Keratong is 3222 points.

Table 1: Database of oil palm trees based on drone images

Study Area	Oil Palm Tree	Non-oil Palm Tree
Jeli	764	608
Keratong	2822	3222

The database consists of training and testing. The oil palm database is divided into a train set and a test set. The train set was a model that classified the image into two categories: oil palm and non-oil palm. The database was analyzed into two categories: 50:50 analysis and 60:40 analysis.

Table 2: Classification of the database of the oil palm tree with 50:50 analysis

Study Area	Category	Oil Palm Tree	Non-oil Palm Tree	Total
Jeli	Training Set	382	304	686
	Testing Set	382	304	686
Keratong	Training Set	1611	1411	3022
	Testing Set	1611	1411	3022

eISSN Number: 3036-017X

3.2 Determination of the Window Size for Classification of Oil Palm Tree Database

Before the accuracy results are obtained from the Support Vector Machine (SVM), the window size needs to be selected. Since the drone was flown at a low altitude in Jeli plantation (Fig. 7), the bigger window was tested. It is tested on different window sizes of 100 x 100 pixels, 150 x 150 pixels, 200 x 200 pixels, and 250 x 250 pixels.

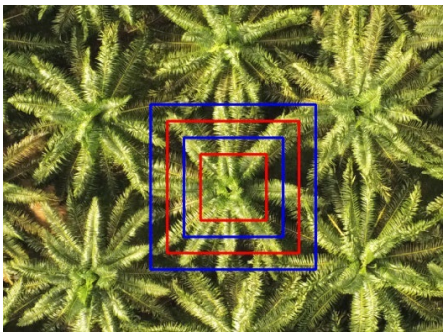

Fig. 7: Different sizes of windows for Jeli Plantation

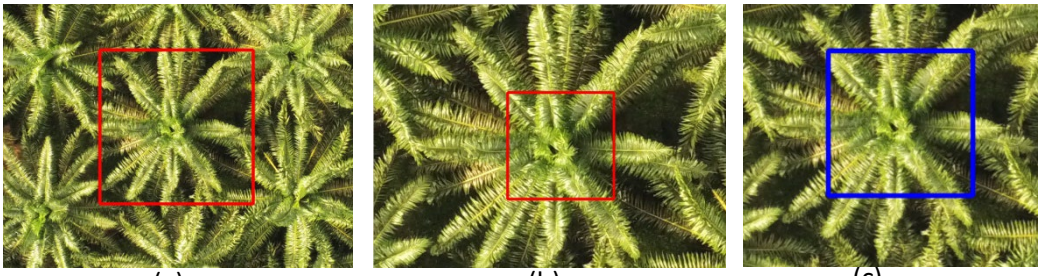

Fig. 8: Oil palm tree in Jeli with window size for (a) 250, (b)100 and (c) 150 pixels.

Fig. 9: Non-oil palm tree with a window size of 250 pixels

Fig. 8 and 9 show a clear image of oil palm and non-oil palm trees in different sizes of windows. In this study area**,** which is Jeli Plantation, 250 x 250 pixels were used. This is because the oil palm crown can be covered on this specific window, and the accuracy of using this window is higher than that of another. A window size of less than 250 may only cover a few parts of the oil palm crown.

For the Keratong plantation, the drone was flown higher compared to the Jeli plantation. Hence, the smaller window was tested to determine the best window for the image. It is tested on different window sizes of 20 x 20 pixels, 40 x 40 pixels, and 100 x 100 pixels.

Fig. 10 clearly represents an oil palm tree in various window sizes at the Keratong plantation. The study area was 40 by 40 pixels in size. This is because this particular window can be used to cover the oil palm crown, and this window has better accuracy than others. While 100 x 100 pixels is too huge for the image of the oil palm crown, windows smaller than 40 may only cover a small portion.

eISSN Number: 3036-017X

(a) (b) (c)

Fig. 10: Oil palm tree in Keratong with window size for (a) 20, (b)40 and (c) 100 pixels.

Given the results (Table 3), it is shown that for both locations, Haar Wavelet recorded a higher accuracy compared to the other algorithms, with 83.75% for Jeli and 86.99% for Keratong. However, there were differences in the window size, as Haar wavelet recorded high accuracy in Jeli for window size 250 x 250 pixels and for window size 44 x 44 pixels in Keratong.

As regards the window size used for every computation for the overall accuracy of each algorithm, the statistic parameter and the offset for the oil palm trees and the non-oil palm trees is 250 x 250 pixels. This is due to the fact that texture features often have poor extraction accuracy using small window sizes, while better accuracy has been seen in larger sizes [27]. This means that an accurate estimate of the population parameter is only obtained when the sample size is large.

Table 3: Overall accuracy for GLCM, wavelet transforms & template matching for different analysis

Study Area	Window Size	Accuracy for Overall GLCM (%)	Accuracy for Wavelet Transform Overall (%)	Accuracy for Template Matching Overall (%)
Jeli	150	54.06	43.57	38.26
	250	49.85	**83.75**	61.30
	300	48.35	51.18	33.28
Keratong	30	79.44	84.81	59.99
	40	76.24	86.90	75.81
	44	72.47	**86.99**	68.20

3.3 Classification Result of Oil Palm Tree Database Based on Drone Images

Based on the results obtained from the Support Vector Machine (SVM), the highest accuracy was achieved using the Wavelet Transform. It is tested on both oil palm and non-oil palm.

Based on Table 4, the wavelet transform algorithm has a value for overall accuracy of 83.75%, 81.77% for oil palm, and 86.18% for non-oil palm. The template matching obtained the highest in accuracy of non-oil palm with 93% but got the lowest accuracy value in oil palm for every window size. Template matching shows the highest due to its wavelet features matching the non-oil palm requirement features.

Table 5 presents the accuracy of different algorithms (GLCM, Haar Wavelet, and Template Matching) in identifying oil palm and non-oil palm areas within the Keratong study area at various window sizes (30, 40, 44). Haar Wavelet consistently shows high accuracy across all categories. GLCM and Template Matching algorithms also perform well but vary more significantly depending on the window size. The accuracy percentages are higher for oil palm identification compared to non-oil palm. The study highlights the potential of advanced drone-based image recognition techniques for optimizing plantation management and contributing to sustainable production practices.

eISSN Number: 3036-017X

Table 4: Overall accuracy for algorithms GLCM, Wavelet Transforms & Template Matching for Jeli

Study Area	Window Size	Type of Algorithms	Accuracy		
			Overall (%)	Oil palm (%)	Non-oil palm (%)
Jeli	150	GLCM	54.06	67.56	37.5
		Haar Wavelet	43.57	31.9	57.89
		Template Matching	38.26	10.72	72.04
	250	GLCM	49.85	39.01	63.49
		Haar Wavelet	**83.75**	81.77	86.18
		Template Matching	61.3	35.39	93
	300	GLCM	48.35	27.91	76.69
		Haar Wavelet	51.18	71.54	23.13
		Template Matching	33.28	5.69	71.27

Table 5: Overall accuracy for algorithms GLCM, Wavelet Transforms & Template Matching for Keratong

Study Area	Window Size	Type of Algorithms	Accuracy		
			Overall (%)	Oil palm (%)	Non-oil palm (%)
Keratong	30	GLCM	79.44	86.83	73.09
		Haar Wavelet	84.81	87.71	81.5
		Template Matching	59.99	32.09	91.85
	40	GLCM	76.24	93.23	56.84
		Haar Wavelet	**86.9**	90.88	82.35
		Template Matching	75.81	61.82	91.78
	44	GLCM	72.47	92.11	50.07
		Haar Wavelet	86.99	91.68	81.63
		Template Matching	68.2	43.6	96.25

From the result, it concluded that the reason why every single parameter was changed was to see the difference and the implications on the number of trees detected. For GLCM, the statistical parameters include contrast, correlation, dissimilarity, energy, entropy, homogeneity, mean, and variance.

Table 6 shows that for window size 300x 300 pixels, the highest accuracy overall is from the correlation parameter, which is 57.01%. and 81.84% for oil palm accuracy. However, for non-oil palm accuracy, Correlation recorded the lowest accuracy with 22.56%. As for the window size of 250x250 pixels, Dissimilarity recorded the highest accuracy with 51.17% overall. Three parameters recorded a zero reading for oil palm accuracy and 100 % accuracy for non-oil palm, which are Energy, Entropy, and Mean.

This statistic can also be used to measure every category for the oil palm tree. Correlation, entropy, and homogeneity can be alternatives in order to increase the accuracy [28]. Basically, there are three algorithms used for analyzing the oil palm tree recognition. There are Gray-Level Co-Occurrence Matrix (GLCM), Haar Wavelet and Template Matching. These three algorithms provide different accuracy values for each of them. In addition, there are also eight statistical parameters, including Contrast Analysis (CON), Correlation (CORR), Dissimilarity (DISS), Energy (ENE), Entropy (ENT), Homogeneity (HOM), Mean (MEAN) Variance (VAR), and offset can be adjusted to identify the data accuracy. Besides that, the reason why this study used 250 window sizes is to get more precise and clear images of oil palms. The high-resolution images of oil palms really help in distinguishing between one and another trees.

eISSN Number: 3036-017X

Window size 250 x 250 pixels helps to cover the whole crown of the oil palm compared to the size of a window less than 250 x 250 pixels, where they only cover half of the crown.

Table 6: Overall accuracy for statistics parameter in Jeli plantation

Study Area	Window Size	Statistic Parameter	Overall Accuracy (%)	Oil Palm Accuracy (%)	Non-Oil Palm Accuracy (%)
Jeli	150	**Contrast**	47.27	18.77	82.24
		Correlation	45.79	10.72	88.82
		Energy	44.9	0	100
		Homogeneity	**51.26**	84.72	10.2
		Dissimilarity	45.64	47.18	43.75
		Entropy	44.9	0	100
		Mean	48.3	47.45	49.34
		Variance	46.09	27.88	68.42
	250	**Contrast**	47.67	18.85	83.88
		Correlation	45.63	4.45	97.37
		Energy	44.31	0	100
		Homogeneity	50.29	71.47	23.68
		Dissimilarity	**51.17**	36.91	69.08
		Entropy	44.31	0	100
		Mean	44.31	0	100
		Variance	44.9	10.99	87.5
	300	**Contrast**	43.15	5.42	95.49
		Correlation	**57.01**	81.84	22.56
		Energy	41.73	0	99.62
		Homogeneity	42.68	8.94	89.47
		Dissimilarity	41.73	0	99.62
		Entropy	41.73	0	99.62
		Mean	41.73	0	99.62
		Variance	45.5	10.84	93.61

Table 7 depicts a comparison of the accuracy of various parameters for window sizes 30, 40, and 44. Window size 40 recorded the highest accuracy among the other window sizes, with 62.96% for parameter Variance. For window size 30, contrast recorded the highest overall accuracy, and 59.86% was recorded for window size 40. For Keratong, the study used a window size of 40 x 40 pixels to obtain more precise and clear images of oil palm trees. High-resolution images help distinguish between individual trees. Window sizes less than 40 x 40 pixels only cover half of the crown of oil palm trees.

eISSN Number: 3036-017X

Table 7: Overall accuracy for statistics parameter in Keratong plantation

Study Area	Window Size	Statistic Parameter	Overall Accuracy (%)	Oil Palm Accuracy (%)	Non-Oil Palm Accuracy (%)
KERATONG	30	**Contrast**	**64.18**	27.08	96.1
		Correlation	57.1	69.88	46.1
		Energy	53.71	0	99.33
		Homogeneity	63.84	79.01	50.78
		Dissimilarity	53.71	0	99.93
		Entropy	53.71	0	99.93
		Mean	53.71	0	99.93
		Variance	58.28	11.11	98.87
	40	**Contrast**	62.11	43.7	83.13
		Correlation	52.15	34.89	71.86
		Energy	46.69	0	100
		Homogeneity	60.36	83.67	33.73
		Dissimilarity	46.99	0.56	100
		Entropy	46.69	0	100
		Mean	47.35	1.74	99.43
		Variance	**62.97**	48.85	79.09
	44	**Contrast**	**59.86**	43.73	78.26
		Correlation	50.2	19.69	84.99
		Energy	46.69	0	99.93
		Homogeneity	59.76	76.46	40.72
		Dissimilarity	46.69	0	99.93
		Entropy	46.69	0	99.93
		Mean	46.69	0	99.93
		Variance	58.24	33.04	86.97

4. Conclusion

This research study has shown a method that does no harm to the oil palm and facilitates the user to practice the recognition technique on the tree. The algorithms, including Gray Level Co-Occurrence Matrix (GLCM), Haar Wavelet, and Template Matching, provide a good assist in getting the accuracy of the data. Haar Wavelet proves this algorithm can give the highest value on overall accuracy. The other eight statistic parameters can also be used to manipulate the GLCM, while offset parameters can improve accuracy so that users can also apply the algorithm to other applications or methods. High spatial resolution imagery is ideal for use in this area, allowing the researchers to clearly see the size and pattern of the oil palm tree crown.

References

[1] Malaysian Palm Oil Council and Malaysian Palm Oil Board. Fact Sheets: Malaysian Palm Oil. Selangor, Malaysia. 2008.

[2] Mansur MA, Mukhtar RB, Doksi JA. The Usefulness of Unmanned Aerial Vehicle (UAV) Imagery for Automated Palm Oil Tree Counting. J Forestry, 2014;1(1):1-6.

eISSN Number: 3036-017X

[3] Srestasathiern P, Rakwatin P. Oil palm tree detection with high resolution multi-spectral satellite imagery. Remote Sens, 2014;6(10):9749-9774.
[4] Kattenborn T, Sperlich M, Bataua K, Koch B. Automatic single tree detection in plantations using UAV-based photogrammetric point clouds. Int Arch Photogramm Remote Sens Spat Inf Sci, 2014;40(3):139.
[5] Shafri HZ, Hamdan N, Saripan MI. Semi-automatic detection and counting of oil palm trees from high spatial resolution airborne imagery. Int J Remote Sens, 2011;32(8):2095-2115.
[6] Szantoi Z, Malone S, Escobedo F, Misas O, Smith S, Dewitt B. A tool for rapid post-hurricane urban tree debris estimates using high resolution aerial imagery. Int J Appl Earth Obs Geoinf, 2012;18:548-556.
[7] Katoh M, Gougeon FA. Improving the precision of tree counting by combining tree detection with crown delineation and classification on homogeneity guided smoothed high resolution (50 cm) multispectral airborne digital data. Remote Sens, 2012;4(5):1411-1424.
[8] Bazi Y, Malek S, Alajlan N, AlHichri H. An automatic approach for palm tree counting in UAV images. IEEE Geosci Remote Sens Symp, 2014;537-540.
[9] Gong X, Wei D, Zhou G. Extracting trees and structure parameters via integration of LIDAR data and ground imagery. IEEE Int Geosci Remote Sens Symp, 2010;2703-2706.
[10] Christophe E, Inglada J. Object counting in high resolution remote sensing images with OTB. IEEE Int Geosci Remote Sens Symp, 2009;Vol. 4, IV-737.
[11] Vibha L, Shenoy PD, Venugopal KR, Patnaik LM. Robust technique for segmentation and counting of trees from remotely sensed data. IEEE Int Adv Comput Conf, 2009;1437-1442.
[12] Li W, Fu H, Yu L, Cracknell A. Deep learning based oil palm tree detection and counting for high-resolution remote sensing images. Remote Sens, 2017;9(1):22.
[13] Mubin NA, Nadarajoo E, Shafri HZM, Hamedianfar A. Young and mature oil palm tree detection and counting using convolutional neural network deep learning method. Int J Remote Sens, 2019;40(19):7500-7515.
[14] Ayisy Y. Malaysia to cap 6.5m ha of oil palm plantations by 2023. News Straits Times, 2019.
[15] Ismail A, Ahmad S M, Sharudin SZ. Labour productivity in the Malaysian oil palm plantation sector. Oil Palm Ind Econ J, 2015;15(2):1-10.
[16] Canada Centre for Remote Sensing/Natural Resources Canada. GlobeSAR2 Radar Image Processing and Information Extraction Workbook Version 1.2. Ottawa, Ontario, Canada, 1997.
[17] Lillesand T, Kiefer RW, Chipman J. Remote sensing and image interpretation. John Wiley Sons, 2015.
[18] Greenwood WW, Lynch JP, Zekkos D. Applications of UAVs in civil infrastructure. J Infrastruct Syst, 2019;25(2).
[19] Ambati PR, Padhi R. Robust auto-landing of fixed-wing UAVs using neuro-adaptive design. Control Eng Pract, 2017;60:218-232.
[20] Ojala T, Pietikäinen M. Texture classification. CVonline: The Evolving, Distributed, Non-Proprietary, On-Line Compendium of Computer Vision, 2001.
[21] Singh S, Srivastava D, Agarwal S. GLCM and its application in pattern recognition. IEEE Int Symp Comput Bus Intell, 2017;20-25.
[22] Hall-Beyer M. GLCM texture: a tutorial v. 3.0, 2017.
[23] Luces R A. Template-based versus Feature-based Template Matching. Medium, 2019.
[24] Jiao L, Liang M, Chen H, Yang S, Liu H, Cao X. Deep Fully Convolutional Network-Based Spatial Distribution Prediction for Hyperspectral Image Classification. IEEE Trans Geosci Remote Sens, 2017;55:5585-5599.
[25] Lagkas T, Argyriou V, Bibi S, Sarigiannidis P. UAV IoT framework views and challenges: towards protecting drones as “things”. Sensors, 2018;18(11):4015.
[26] Omasa K, Hosoi F, Konishi A. 3D LIDAR imaging for detecting and understanding plant responses and canopy structure. J Exp Bot, 2007;58:881-898.
[27] Daliman S, Syed Abdul Rahman S A, Ibrahim B. Segmentation of Oil Palm Area Based on GLCM-SVM and NDVI. IEEE Region 10 Tech Symp, 2014;14-16 April, Berjaya Times Square Hotel, Kuala Lumpur, Malaysia, 2014.
[28] Yayusman LF, Nagasawa R. Identification of Smallholders’ Oil Palm Plantations Using Alos Data (A Case Study In Lampung Province, Indonesia). Asian Conf Remote Sens, 2015.

eISSN Number: 3036-017X